Global Change Biology

Global Change Biology (2011) **17**, 3608–3619, doi: 10.1111/j.1365-2486.2011.02486.x

Using a climatic niche model to predict the direct and indirect impacts of climate change on the distribution of Douglas-fir in New Zealand

MICHAEL S. WATT*, JEFFREY K. STONE†, IAN A. HOOD‡ and LUCY K. MANNING§

Scion, PO Box 29237, Christchurch, 8540, New Zealand, †Department of Botany and Plant Pathology, Oregon State University, Corvallis, OR, 97331, USA, ‡Scion Forest Biosecurity and Protection, Private Bag 3020, Rotorua, 3046, New Zealand, §Boffa Miskell, PO Box 13 373, Tauranga, 3141, New Zealand

Abstract

Climate change is likely to have major impacts on the distribution of planted and natural forests. Herein, we demonstrate how a process-based niche model (CLIMEX) can be extended to globally project the potential habitat suitable for Douglas-fir. Within this distribution, we use CLIMEX to predict abundance of the pathogen *Phaeocryptopus gaeumannii* and severity of its associated foliage disease, Swiss needle cast. The distribution and severity of the disease, which can strongly reduce growth rate of Douglas-fir, is closely correlated with seasonal temperatures and precipitation. This model is used to project how climate change during the 2080s may alter the area suitable for Douglas-fir plantations within New Zealand. The climate change scenarios used indicate that the land area suitable for Douglas-fir production in the North Island will be reduced markedly from near 100% under current climate to 36–64% of the total land area by 2080s. Within areas shown to be suitable for the host in the North Island, four of the six climate change scenarios predict substantial increases in disease severity that will make these regions at best marginal for Douglas-fir by the 2080s. In contrast, most regions in the South Island are projected to sustain relatively low levels of disease, and remain suitable for Douglas-fir under climate change over the course of this century.

Keywords: biological invasions, biosecurity, CLIMEX, ecological niche model, invasive alien species, pest risk mapping, predictive modelling

Received 31 December 2010 and accepted 12 June 2011

Introduction

Climate has long been recognized as an important environmental determinant in the distribution of pathogens and development of disease (Wallin & Waggoner, 1950; De Wolf & Isard, 2007). This is particularly the case for plant pathogens, where air temperature has been shown to influence their growth and cold season survival, whereas rainfall can strongly affect their ability to disperse and infect their hosts (Coakley *et al*., 1999; De Wolf & Isard, 2007). Process-based niche models, such as CLIMEX, have utilized the relationship between climate and disease presence to project potential distribution of a wide range of invasive plant pathogens and disease (Brasier & Scott, 1994; Lanoiselet *et al*., 2002; Yonow *et al*., 2004; Paul *et al*., 2005; Venette & Cohen, 2006; Desprez-Loustau *et al*., 2007; Ganley *et al*., 2009; Watt *et al*., 2009). However, to date, process-based niche models have not been used to predict spatial and temporal variation in disease severity, and impacts on the host within areas delineated as suitable for both host and disease.

Developing models that can account for the effects of climate on disease severity is particularly important for ecosystems encompassing wide variation in host and pathogen lifecycles, as occuring in both natural and plantation forests. Microbial pathogens have shorter generation times than trees, and so their populations can be expected to respond more rapidly to climate change. Consequently, forests at low risk at the time of establishment may be susceptible to greater risk after several decades, if rapidly changing climate renders the environment more favourable for pathogen growth and reproduction.

Development of process-based models that can predict disease severity and host impacts within a framework that constrains the spatial extent of host and disease distribution would represent a major advance. This type of model would allow the impact of climate change to be partitioned into the direct impacts on the host and indirect effects on the host via the disease. Herein, we used the Douglas-fir – Swiss needle cast pathosystem to illustrate how such a process-based model could be developed.

Correspondence: Michael S. Watt, tel. +64 3 364 2949, fax +64 3 364 2812, e-mail: michael.watt@scionresearch.com

Swiss needle cast is a foliage disease caused by the ascomycete *Phaeocryptopus gaeumannii* (Rohde) Petrak, which occurs naturally in indigenous *Pseudotsuga menziesii* (Mirb.) Franco (Douglas-fir) in western North America (Boyce, 1940). The fungus was initially discovered and described from diseased Douglas-fir plantations in Switzerland in 1925, and soon afterward reported from other locations in Europe (Boyce, 1940). Infection by this fungus frequently results in chlorotic foliage, defoliation and growth reduction (Boyce, 1940). Outbreaks of Swiss needle cast have occurred in both native and plantation grown *P. menziesii* in the Pacific Northwest (Hansen *et al*., 2000; Manter *et al*., 2005; Stone *et al*., 2008b) and forest plantations in Europe and the United Kingdom (Boyce, 1940; Peace, 1962), the northeastern United States (Morton & Patton, 1970), Turkey (Temel *et al*., 2003), Australia (Marks *et al*., 1989) and New Zealand (Hood *et al*., 1990).

As there is a physiological basis linking pathogen abundance to disease severity, the *P. menziesii*/*P. gaeumannii* association provides a useful case study for development of an integrated model system. Fruiting bodies (pseudothecia) of *P. gauemannii* physically occlude the stomata of Douglas-fir needles, thereby impairing gas exchange and photosynthesis (Manter *et al*., 2003). The physical obstruction of stomata is considered the mechanism of pathogenicity, as cellular disruption or toxins typical of some plant diseases are absent from this pathosystem (Manter *et al*., 2003; Stone *et al*., 2008a). The premature loss of foliage and resulting growth reductions in *P. menziesii* are thus directly related to reduction in CO_2 assimilation that in turn is directly related to the abundance of the pathogen (Manter *et al*., 2003). Pathogen abundance and disease severity can be quantified, respectively, from pathogen pseudothecial frequency and host needle retention; both have been shown to increase under warm winter air temperatures and prolonged periods of spring leaf wetness (Manter *et al*., 2005; Stone *et al*., 2007). This relationship between pathogen abundance and host needle retention has been convincingly demonstrated in both Oregon and New Zealand (Hood & Kimberley, 2005; Stone *et al*., 2007, 2008a; Watt *et al*., 2010).

Given the responsiveness of the pathogen to air temperature, climate change is likely to have a marked effect on disease severity and host productivity. Both the disease and host co-occur over large contiguous temperate regions, and there is potential for the distribution of the host and severity of the disease to differentially expand or recede under climate change. Under environmental conditions favourable to the pathogen, the disease has been shown to result in volume reductions in *P. menziesii* of up to 50% (Maguire *et al*., 2002), with losses of ca. 30% typically reported in both native forests (Maguire *et al*., 2002; Black *et al*., 2010) and exotic stands (Kimberley *et al*., 2011). Severe disease in Douglas-fir forest plantations in western Oregon has commonly resulted in replacement of the normally faster growing Douglas-fir by natural regeneration of competing species such as western hemlock [*Tsuga heterophylla* (Raf.) Sarg.] that is not susceptible to the disease (Hansen *et al*., 2000).

Herein, we parameterize the process-based distribution model CLIMEX to project the potential distribution of *P. menziesii* and Swiss needle cast. Using detailed measurements collected across a broad environmental gradient within New Zealand, we fit a set of functions within CLIMEX to describe spatial variation in *P. gauemannii* abundance and *P. menziesii* foliage retention within this potential distribution. The parameterized model is then used to project potential distribution of Douglas-fir, pathogen abundance and disease severity under current and future climate within New Zealand. We discuss the utility of this case study as a generic approach for identifying impacts of diseases on the future distribution of key tree species.

Methods

Disease and pathogen records

Reported observations of Swiss needle cast or *P. gauemannii* were compiled using individual point, county or state locations. A full description of countries in which the disease or pathogen has been found are given in Supplementary material 1, and references used to compile these locations are given in Supplementary material 2. In summary, disease and pathogen locations were obtained for the following countries in Europe and Eurasia: Austria, Belgium, Bulgaria, Czech Republic, Denmark, England, Germany, Finland, Hungary, Ireland, Italy, Latvia, Netherlands, Portugal, Romania, Scotland, Slovenia, Sweden, Switzerland, Turkey and Wales. Within the Americas, the disease and pathogen has been found in Canada, United States, Mexico and Chile, while in Australasia, records were obtained from Australia and New Zealand.

The CLIMEX model

CLIMEX is a dynamic model that integrates modelled weekly responses of a population to climate to create a series of annual indices (Sutherst *et al*., 2007). CLIMEX uses an annual growth index (GI_A) to describe the potential for population growth as a function of soil moisture and temperature during favourable conditions, and up to eight stress indices (SI) to simulate the ability of the population to survive unfavourable conditions. The following two sections describe the generic fitting of CLIMEX and underlying theory behind indices. For more details on theory and mathematics of functions within CLIMEX, readers are referred to Sutherst & Maywald (1985) and Sutherst *et al*. (2007).

Growth index

Growth index of the pathogen is determined from the temperature and moisture indices. For both indices, cardinal values (see Table 1 for parameters) are specified for a three-segment linear approximation of a Stinner or Pradhan equation (Pradhan, 1946; Stinner *et al*., 1974). This function uses parameter values to describe the minimum value suitable for any growth (DV0 for temperature and SM0 for soil moisture), the minimum (DV1 or SM1) and maximum value (DV2 or SM2) for optimal growth rates and the maximum value for any growth (DV3 or SM3). The product of the temperature index and moisture index (TI_w and MI_w) are then calculated to evaluate the climatic suitability of each week. These weekly values are then integrated to describe the GI_A, as,

$$GI_A = \frac{100}{52}\sum_{w=1}^{52} TI_w MI_w, \quad (1)$$

which ranges from 0 for sites with no growth to 100 for sites that are optimal for growth.

Ecoclimatic index

The SI and stress interaction index (SX) predominantly define the potential climatically suitable spatial range of a species and scale from 0 to infinity, with 0 describing no stress and values exceeding 100 describing lethal conditions. The SI are defined by up to four stresses that include cold stress (CS), heat stress (HS), dry stress (DS) and wet stress (WS). The four interactions between these define the SX that can include cold dry stress (CDX), cold wet stress (CWX), hot-dry stress (HDX) and hot-wet stress (HWX). Each of the eight SI is described by a function with parameters that define the starting threshold soil moisture or temperature (or both in the case of stress interactions) and a rate of linear accumulation, for the stress, either above or below the threshold starting point. Usually, not all of the eight SI and SX are required to describe the species distribution. The SI (Eqn 2) and SX (Eqn 3) are determined weekly and expressed over an annual period, respectively, from,

$$SI = \left[\left(1-\frac{CS}{100}\right)\left(1-\frac{HS}{100}\right)\left(1-\frac{DS}{100}\right)\left(1-\frac{WS}{100}\right)\right]. \quad (2)$$

$$SX = \left[\left(1-\frac{CDX}{100}\right)\left(1-\frac{CWX}{100}\right)\left(1-\frac{HDX}{100}\right)\left(1-\frac{HWX}{100}\right)\right]. \quad (3)$$

Ecoclimatic index, EI, is defined as $EI = SI \times SX \times GI_A$ and ranges from 0 for locations at which the species is not able to persist to 100 for locations that are optimal for the species.

CLIMEX model fitting to Douglas-fir – Swiss needle cast pathosystem

Using distribution records for *P. gaeumannii*, we found that the pathogen is capable of occurring under virtually all environmental conditions found throughout the host range. Specifically, the disease is found at the coldest (most northern) and

Table 1 CLIMEX parameters for Swiss needle cast. For the moisture indices field capacity occurs at a value of 1.0

Index	Parameter	Values*
Temperature	DV0 = lower threshold	10.0 °C
	DV1 = lower optimum temperature	20.0 °C
	DV2 = upper optimum temperature	21.0 °C
	DV3 = upper threshold	28 °C
Moisture	SM0 = lower soil moisture threshold	0.11
	SM1 = lower optimum soil moisture	0.8
	SM2 = upper optimum soil moisture	1.5
	SM3 = upper soil moisture threshold	1.7
Cold stress	TTCS = temperature threshold	−16.0 °C
	THCS = stress accumulation rate	−0.01 week^{-1}
	DTCS = degree-day threshold	1.0 °C days
	DHCS = degree-day stress accumulation rate	−0.00005 week^{-1}
Heat stress	TTHS = temperature threshold	28.0 °C
	THHS = stress accumulation rate	0.003 week^{-1}
Dry stress	SMDS = soil moisture dry stress threshold	0.11
	HDS = stress accumulation rate	−0.01 week^{-1}
Hot-dry stress	TTHD = hot-dry temperature threshold	20 °C
	MTHD = hot-dry soil moisture threshold	0.11
	PHD = stress accumulation rate	0.04 week^{-1}
Hot-wet stress	TTHW = hot-wet temperature threshold	23 °C
	MTHW = hot-wet soil moisture threshold	0.9
	PHW = stress accumulation rate	0.05 week^{-1}

*Values without units are dimensionless indices.

hottest (most southern) natural range of the host (Fig. 1). A single CLIMEX model was deemed to be suitable for modelling the two species, as GI and SI could be partitioned between the two species to describe the most limiting parts of the system. SI were used to describe the distribution of the host, whereas GI were used to describe the abundance of the pathogen and severity of the disease. SI are not limiting for the disease distribution, as the disease was found to occur across the host range. As disease severity strongly affects both growth rate and distribution of the host, it makes more sense to link GI directly to disease severity, rather than host development.

The following categorization was used to describe host presence, pathogen abundance and disease severity as a function of EI and GI: (i) at EI = 0 climatic conditions are not suitable for the host, so neither the pathogen or disease will occur, (ii) at EI > 0 and low values of GI (GI < 6 in this study) the host will occur, and consequently the pathogen will be present, but little disease expression will occur, and (iii) at EI > 0 and higher values of GI (GI $\geq$ 6), both host and pathogen will be present and the disease will be expressed, with disease severity scaling positively with GI. The climate dataset used for the parameter fitting was a 0.5° of arc dataset generated by Kriticos *et al.* (2006) from the 1961 to 1990 climate normals provided by the climate research unit (Mitchell *et al.*, 2004).

Fitting SI to model host distribution

An iterative approach was used to fit the SI to the known distribution of the host in the native range of North America. The accuracy of the resulting model was tested against independent observations from the known exotic pathogen and disease range in Europe, South America, Australia and New Zealand.

Examination of the pathogen and disease records in North America showed that these largely encompassed the very wide native distribution of the two subspecies (ssp. *menziesii* and ssp. *glauca*) of Douglas-fir (Fig. 1). CS (Table 1) was used to limit the projected distribution of the host in northern and eastern British Columbia to observed limits (Fig. 1). Similarly, DS, HS and HDX were set to physiologically reasonable values (Table 1) that limited the potential southern distribution of the host to known locations in New Mexico, Arizona and Mexico. These three stresses were used to largely exclude the potential distribution from central and southern California

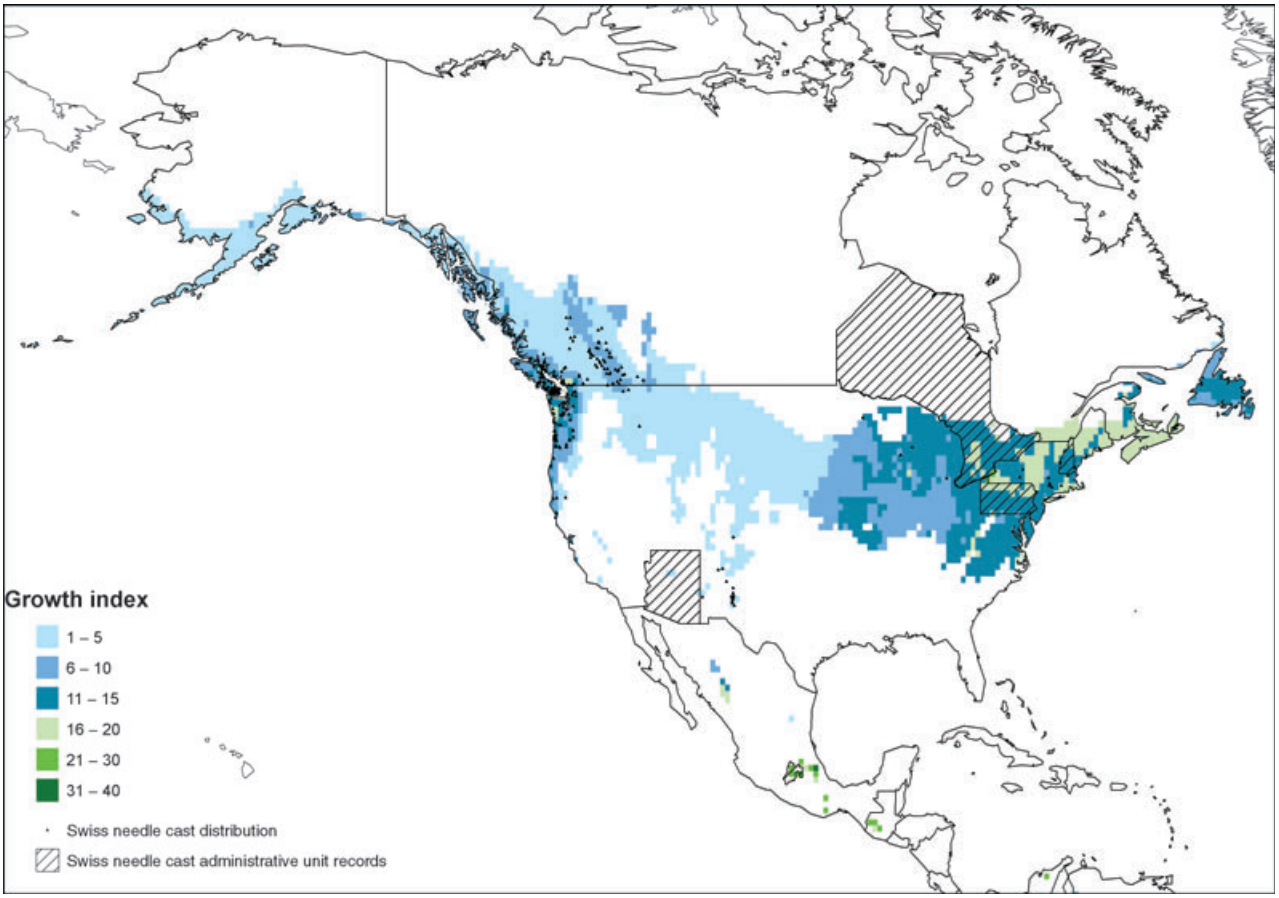

Fig. 1 Map of North America showing the distribution of growth index, GI_A, for regions with ecoclimatic index, EI, >0. Areas shown as white are unsuitable (EI = 0) for the disease and host. Also shown is the distribution of Swiss needle cast, shown as point locations (solid triangles) and provincial records (cross-hatched areas), in which at least one observation has been recorded.

(Fig. 1), where *P. menziesii* is limited to the northern Sierra and Coast Range. Native stands of the less widely distributed, but susceptible, host bigcone Douglas-fir (*P. macrocarpa*) occur in southern California. Although planted bigcone Douglas-fir has been found infected in British Columbia (Pennycook, 1989), neither the pathogen nor the disease have been noted on this species within California (I. Hood, J. Stone, personal observation). We inferred from this observation that environmental limits of the disease are reached around the range of Douglas-fir in California. Following previous research (Wharton & Kriticos, 2004), HWX was used to limit the planted distribution of the coniferous host from warm humid regions in the south-eastern United States. As the host occurs in cool wet environments in the coastal Pacific Northwest (rainfall of 3400 mm yr^{-1}), no WS was used in the model.

The resulting model predicted all but four observations of the pathogen to have a suitable climate (EI $\geq$ 1) for persistence (Fig. 1). Exceptions where suitable climate was not predicted were located at range margins in New Mexico, with low rainfall, and in eastern British Columbia, with very low

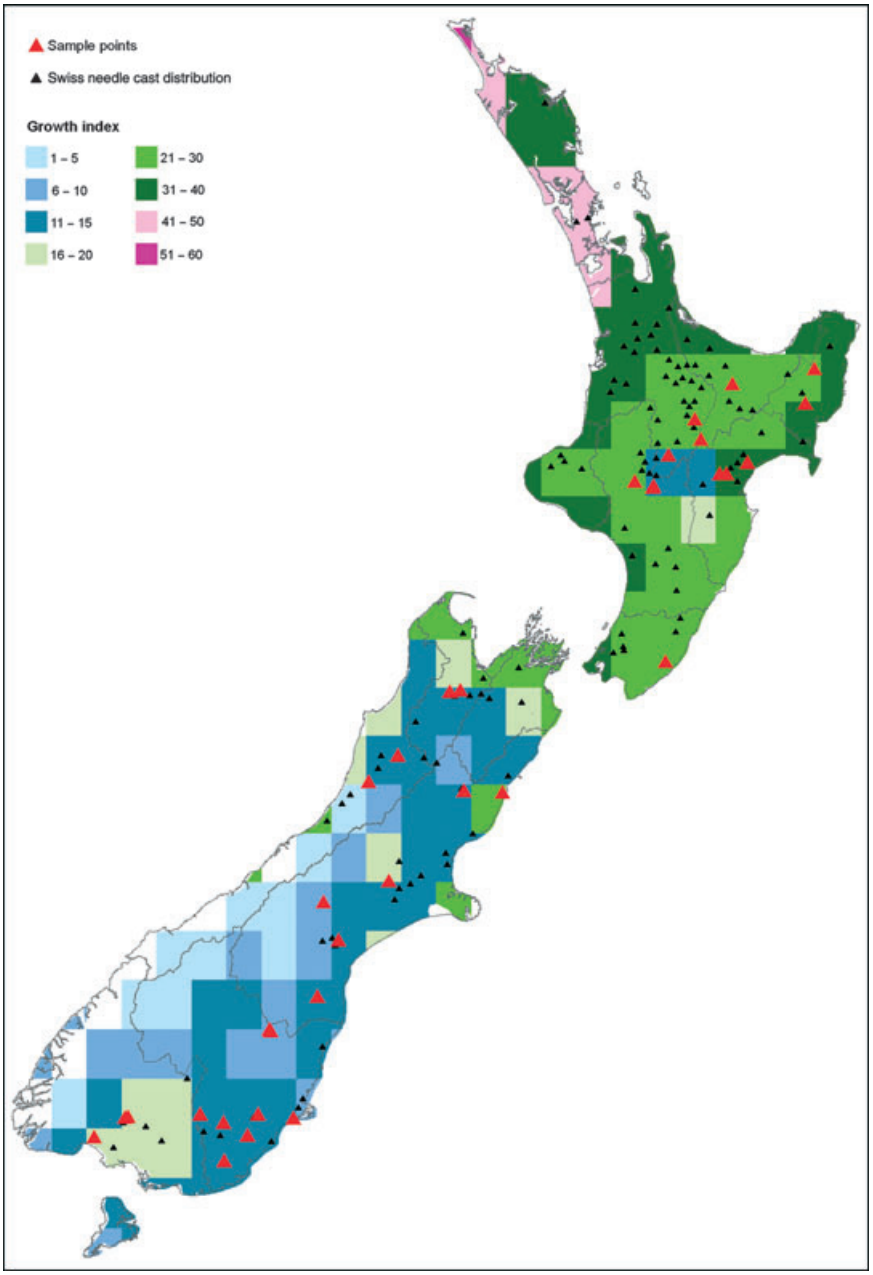

Fig. 2 Map of New Zealand showing the distribution of growth index, GI_A, for regions with ecoclimatic index, EI, >0. Areas shown as white are unsuitable (EI = 0) for the disease and host. Also shown is the distribution of Swiss needle cast, shown as point locations (solid triangles), and sites from which intensive measurements of pathogen abundance and foliage retention were made (red triangles).

winter temperature. All of these locations occurred in dissected terrain, and therefore it is likely that these misfits were attributable to microclimatic variation not captured by the relatively coarse resolution dataset used. All of the records of disease or pathogen, apart from one, in the validation dataset were correctly predicted as occurring in a climate suitable for the pathogen (Fig. S1 for world; Fig. 2 for New Zealand Fig. 3 for Europe). This misfit also occurred in mountainous terrain in eastern Portugal, and as a result the misclassification is likely to be attributable to variation in local climate, from that predicted at a 0.5° resolution (Fig. 3). Notably, the model correctly predicted the distribution of the disease within Australia (see Supplementary information text 1) and Chile within South America (see Fig. S1).

Fitting GI to model pathogen abundance and disease severity

Experimental data. Measurements of pathogen abundance and host needle retention of infected stands were used to iteratively parameterize the functions describing GI. These measurements were taken from mature stands of Douglas-fir across 34 sites covering a wide environmental gradient in New Zealand (see Fig. 2). The sampling methodology used to collect these data is fully described in Stone *et al.* (2007) and briefly outlined below.

At each site, at least 10 trees were randomly selected to represent conditions typical of the site. Healthy *P. menziesii* ssp. *menziesii* (coastal form Douglas-fir) typically retain needles on the internodes produced during the past 4 years, whereas diseased trees lose needles primarily in the older needle cohorts (Hood *et al.*, 1990; Hansen *et al.*, 2000). Per cent foliage retention was visually estimated on secondary branches from the fifth whorl below the apical shoot. The per cent foliage retention of each of the four internodes below the terminal bud, that is, foliage aged from 1 to 4 years at the time of sampling (current-year, newly emerged shoots were excluded), was estimated and averaged for two branches per tree. All foliage retention estimates were made by the same observer. Average per cent foliage retention for the four foliage age classes were summed by tree and then rescaled as a total percentage foliage retention, F_{ret}, for analyses.

Foliage samples were returned to the laboratory where the 2-year-old and 1-year-old internodes were separated, needles removed from branchlets and pooled by age class. Following detailed methods described previously (Stone *et al.*, 2007), a colonization index (CI), was determined as the product of the per cent of needles with visible pseudothecia (incidence,

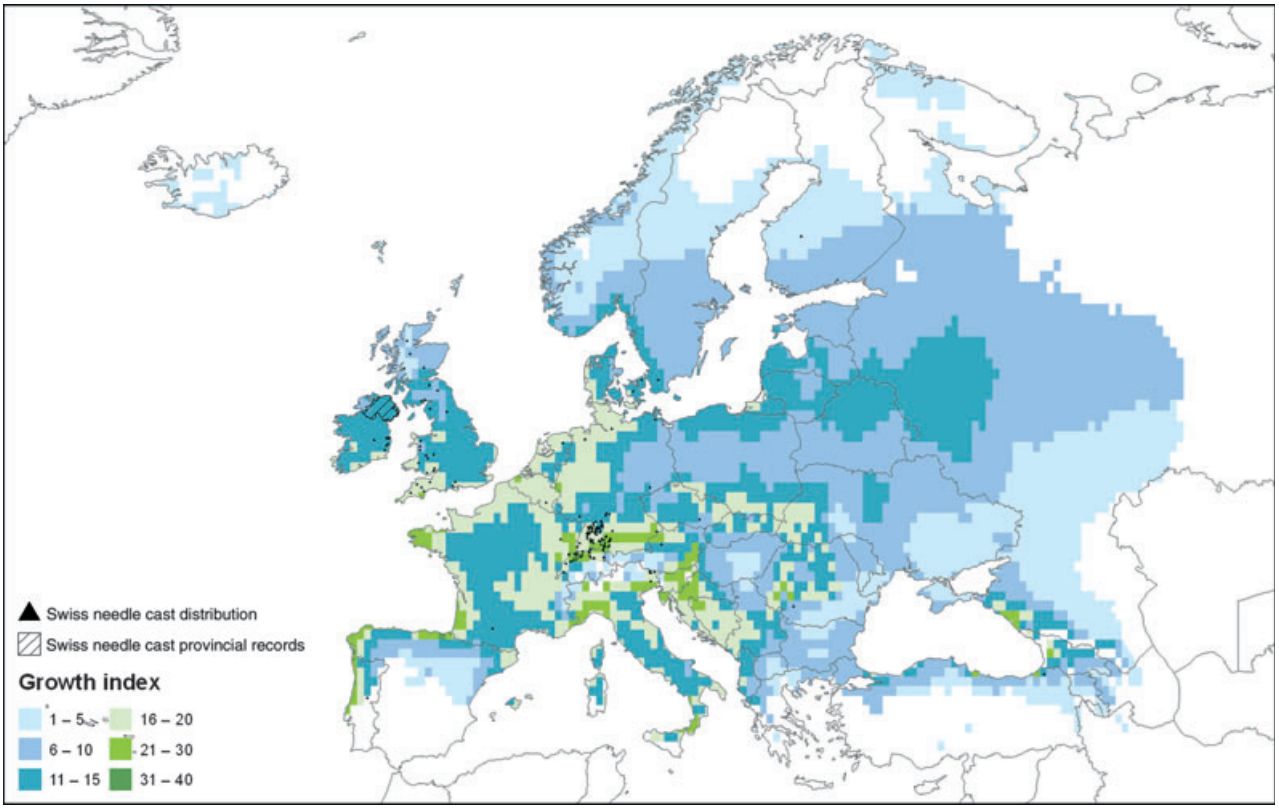

Fig. 3 Map of Europe showing the distribution of growth index, GI_A, for regions with ecoclimatic index, EI, >0. Areas shown as white are unsuitable (EI = 0) for the disease and host. Also shown is the distribution of Swiss needle cast, shown as point locations (solid triangles) and provincial records (cross-hatched areas), in which at least one observation has been recorded.

n = 50) and the average proportion of stomata occluded (pseudothecial density, n = 10). CI was normalized (range from 0 to 1) by needle age, and mean normalized values for each site were determined. These mean normalized values, referred to hereafter as CI_{norm}, were used in all analyses.

Parameter fitting. Parameter values describing TI and MI (Table 1) were iteratively adjusted, within biologically reasonable limits, to most closely match predictions to measurements (described in section above). After, each iteration predictions of GI_A were extracted from CLIMEX and regressed against observations of CI_{norm} and F_{ret}. Analyses were undertaken using SAS (SAS-Institute-Inc., 2000, Cary, NC, USA) using a linear model, with an intercept. GI were repeatedly changed until the coefficient of determination between predictions and observed values was maximized (R^2).

Fitted GI from CLIMEX were significantly ($P < 0.001$) related to both pathogen abundance and foliage retention in New Zealand (Fig. 4). These relationships were linear, accounting for 49% and 61%, respectively, of the variance in CI_{norm} and F_{ret}. Foliage retention was described as a function of CI_{norm} using the following equation:

$$F_{ret} = 108.8 - 1.66GI_A, \quad (4)$$

where values of F_{ret} were constrained to between 0% and 100%.

This relationship shows that for GI_A of between 1 and 5, the pathogen will be present, but CI_{norm} will be sufficiently low that there will be negligible foliage loss (i.e. disease) (Fig. 4). As GI_A increases above 5, increases in CI_{norm} (Fig. 4a) are accompanied by concomitant reductions in F_{ret} (Fig. 4b) that linearly decline from modelled values of 99% to 51%, across a respective range in GI_A of 6–35.

The GI parameters fitted to CI_{norm} and F_{ret} (see Table 1) indicate that pathogen growth sufficient to initiate disease development starts at an interpolated weekly maximum air temperature of 10 °C, increasing to a maximum between 20 and 21 °C, before declining and ceasing at 28 °C. Similarly, development is sensitive to water availability (see Discussion for explanation), with pathogen growth and disease development starting at 11% and increasing to 80% of field capacity. Maximum pathogen growth and disease development is optimal from 80% to 150% of field capacity, before declining, and ceasing at 170% of field capacity (Table 1).

Climate change scenarios. Using the parameterized model, six climate scenarios were used to project potential distribution of Douglas-fir, pathogen abundance and disease severity to the 2080s. These scenarios included the global climate models (GCMs), CSIRO Mark 3.0 (CSIRO, Australia), MIROC-H (Centre for Climate Research, Japan) and NCAR-CCSM

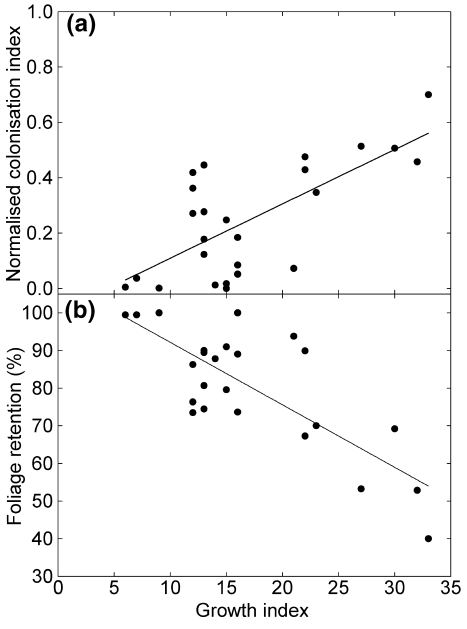

Fig. 4 Relationship between growth index, GI_A, extracted from CLIMEX, and (a) normalized colonization index, CI_{norm}, and (b) foliage retention, F_{ret}. Lines shown fitted to the data include (a) CI_{norm} = 0.087 + 0.0196 GI_A (R^2 = 0.49; $P < 0.001$) and (b) F_{ret} = 108.8–1.66 GI_A (R^2 = 0.61; $P < 0.001$).

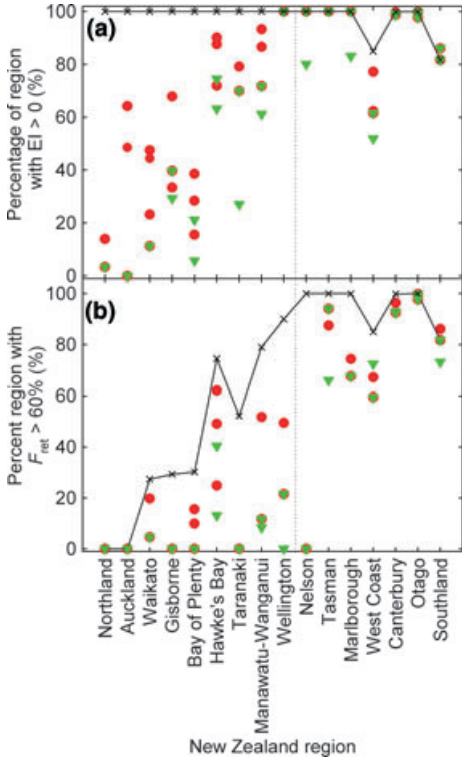

Fig. 5 Variation in the regional percentage area with (a) ecoclimatic index (EI) > 0 and (b) predicted foliage retention (F_{ret}) > 60%, under current (solid line, with crosses), and future climate (symbols). As they represent the extremes, the NCAR and MIROC models forced using the A2 emission scenarios, are shown as filled green triangles, whereas the four other scenarios are shown as filled red circles. Regions are sorted left to right in order of increasing latitude. The dotted line represents the transition point from North Island regions (left) to South Island regions (right).

(National Centre for Atmospheric Research, USA) that were forced using medium (A1B) and high (A2) greenhouse gas emissions. Previous research has shown that CSIRO and MIROC represent the lower and upper extremes in climate change within New Zealand among a broader set of 12 GCMs (Kirschbaum *et al*., 2010). These three GCMs were also selected as they have relatively small horizontal grid spacing and the requisite climatic variables at the monthly resolution required by CLIMEX. The GCM data employed in this project were drawn from the World Climate Research Programmes Coupled Model Intercomparison Project phase 3 multi-model dataset (Meehl *et al*., 2007). Data from these GCMs were pattern-scaled to develop individual change scenarios relative to the base climatology (Whetton *et al*., 2005). The three models cover a range of climate sensitivity, defined as the amount of global warming for a doubling of the atmospheric CO_2 concentration compared with 1990 levels. The respective sensitivities are: CSIRO Mark 3.0 (3.07 °C), NCAR-CCSM (2.70 °C) and MIROC-H (4.30 °C).

Data analysis and model projections

Using the parameterized model, F_{ret} was projected within New Zealand under both current climate and the six climate change scenarios. Projections were constrained to areas where the EI exceeded 0, as these regions are suitable for both host and disease. Areas with a suitable climate (i.e. EI > 0) for the host and disease under both current and future climate were estimated using Regional Council administrative areas with ArcGIS (Redlands, CA, USA).

The displayed projections of F_{ret} under future climate were limited to the three GCMs forced using the A1B emission scenario, because there was less spatial variation between emission scenarios than between GCMs. Differences in F_{ret} between current climate and each of the six climate change scenarios were determined. These differences were spatially displayed for the three A1B scenarios.

Approximately 90% of the current Douglas-fir plantations in New Zealand occurred in areas where predicted F_{ret} under current climate exceeds 60%. Consequently, we used a F_{ret} of 60% as a threshold that demarcates areas suitable ($F_{ret} > 60\%$) and unsuitable ($F_{ret} \leq 60\%$) for commercial plantings. Areas with $F_{ret} > 60\%$ were determined by region under both current and future climate.

Results

Under current climate, the entire North Island was projected to be suitable for Douglas-fir and the pathogen. With the exception of extremely high rainfall areas on the West Coast of the South Island, all of the South Island was projected to be suitable for the host and pathogen (Figs 2 and 5a). All areas on the West Coast in which Douglas-fir is grown, were projected to be suitable (Fig. 2).

Although most of New Zealand was projected to be suitable for the host and pathogen under current climate, there was wide variability in disease impacts as measured by foliage retention (Fig. 6a). Predictions of mean F_{ret} by region show an increase in foliage retention with increasing latitude (North to South), and clearly highlighted the dichotomy between F_{ret} in the North and South Islands (Fig. 6a). In the North Island, regional mean F_{ret} ranged from 37% for Northland to 67% for Wellington, whereas in the South Island, mean regional F_{ret} ranged from 68% for Nelson to 92% for Otago. Regions with greater foliage retention in the North Island were confined to high elevation regions in either central or southern regions (Fig. 6a).

Areas with $F_{ret} > 60\%$ increased with region latitude from nil for Northland and Auckland to 100% in many South Island regions (Fig. 5b). Approximately 90% of current Douglas-fir plantations are located in areas where F_{ret} exceeds 60%, with the majority in the South Island (76%) and a smaller area of plantations in the central North Island (14%).

Effects of climate change on disease distribution and foliage retention

Although the potential distribution of Douglas-fir declines under all future climate scenarios (Fig. 6), these reductions exhibit marked regional variability within New Zealand. Changes in unsuitable area (as described on Fig. 6 by white regions where EI = 0), were most substantial in the North Island. When averaged across all scenarios, proportional reductions in suitable area declined with increasing region latitude, from 93% in Northland to nil in Wellington (Figs 5a and 6b–d). In the South Island, regional changes in areas that were suitable were negligible and <4% for all regions, apart from the West Coast, where average reductions of 26% were predicted (Fig. 5a).

Regional mean changes in suitable areas mask considerable variation between the six climate change scenarios. Variation between the underlying GCMs was greater than that between the emission scenarios. Over the North Island predicted reductions in suitable area for CSIRO were 36% using the A2 (data not shown) and 37% using the A1B emission scenario (Fig. 6b); for NCAR reductions were 47% using the A1B (Fig. 6d) and 57% using the A2 emission scenario (data not shown), whereas for MIROC, reductions were most marked at 57% under the A1B (Fig. 6c) and 64% under the A2 emission scenario (data not shown).

Similarly, projected F_{ret} exhibited considerable variation between regions and climate change scenarios. Compared with current climate, reductions in F_{ret} across all scenarios were greater in the North Island than the South Island, with mean respective reductions in F_{ret} of 11.9% and 9.8% (Fig. 6f–h). Within the North

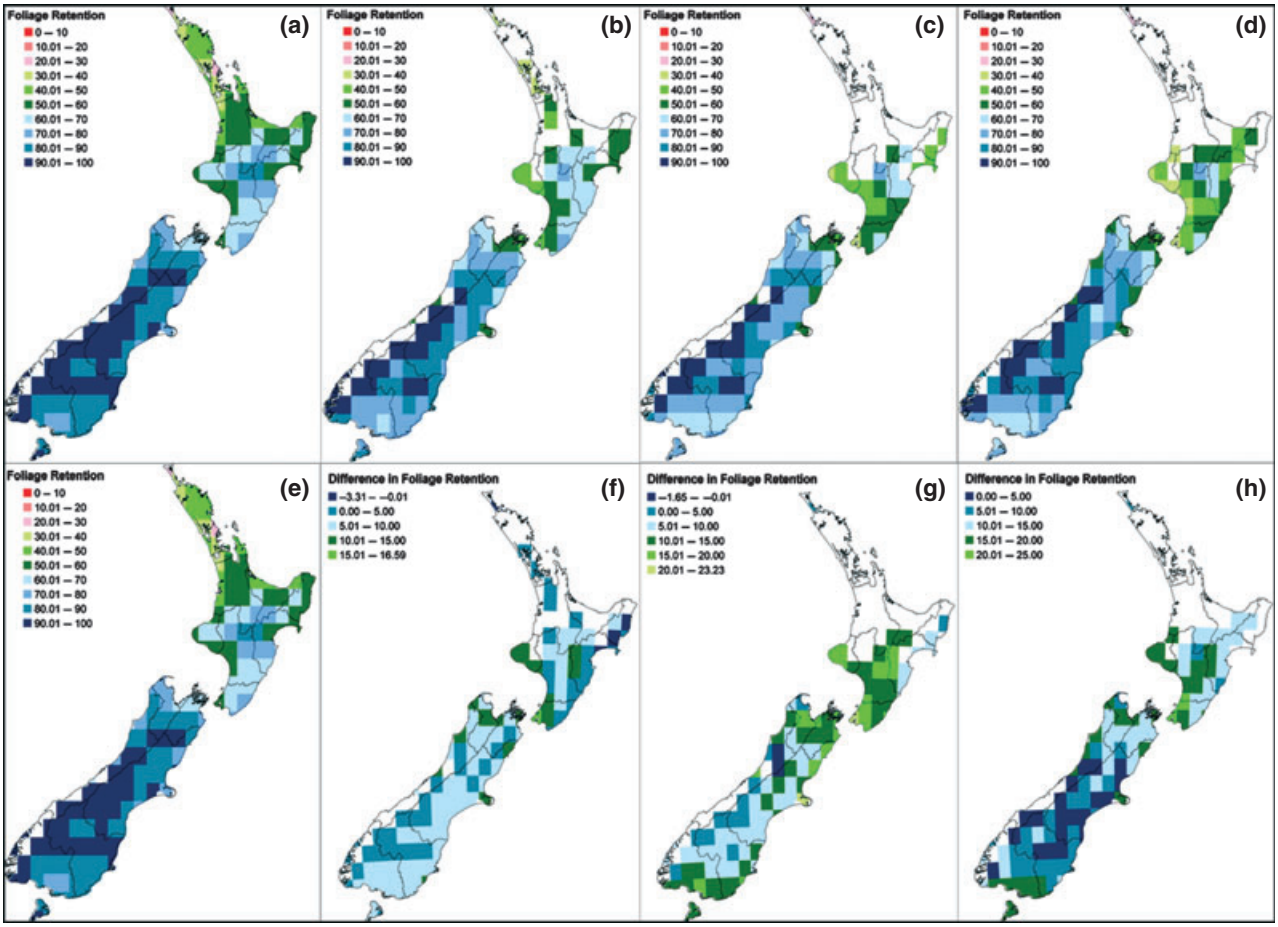

Fig. 6 Spatial variation in foliage retention, F_{ret}, for areas with ecoclimatic index (EI) > 0 under current (a, e) and future climate using the CSIRO (b), MIROC (c) and NCAR (d) GCMs forced using the A1B emissions scenario. Areas shown as white are unsuitable (EI = 0) for the disease or host. Also shown is spatial variation in differences in F_{ret} between current climate and future climate for the CSIRO (f), MIROC (g) and NCAR (h) models. Areas shown as white are unsuitable for the disease or host.

Island, F_{ret} reductions >15% were projected in coastal areas in both the south and west, under NCAR and MIROC (Fig. 5g and h). Losses in F_{ret} of <5% were mainly projected at high altitude in the South Island under all scenarios (Fig. 6f–h).

Most of the variation in F_{ret} between scenarios was attributable to the GCM used. Compared with current climate, losses in F_{ret} were least under the CSIRO model (6.0% North Island; 7.5% South Island), intermediate for MIROC (13.6% North Island; 10.8% South Island) and highest for the NCAR model (16.1% North Island; 11.1% South Island). Less of the variation was attributable to the emission scenario used, with the mean projected losses in F_{ret} greater under the A2 than the A1B emission scenarios within both the North (12.2% vs. 11.6%) and South Island (10.3% vs. 9.4%).

These variations in F_{ret} also reflected changes in area with F_{ret} > 60%. Within the South Island, areas with F_{ret} > 60% changed very little from current climate, with reductions in area ranging from 7% to 11% between scenarios (Fig. 5b). However, in the North Island there was substantial reduction in area with F_{ret} > 60% and a wide range in the magnitude of this reduction between scenarios (Fig. 5b). Projected reductions in land area with F_{ret} > 60% were lowest under CSIRO at 40% using both the A1B (Fig. 6b) and A2 emission scenarios, intermediate for MIROC with reductions of 74% under the A1B emission scenario (Fig. 6d) and 82% under the A2 emission scenario, and most marked for NCAR with projected reductions of 83% using the A1B emission scenario (Fig. 6c) and 87% using the A2 emission scenario.

Discussion

The presented model demonstrates an integrated method for predicting the effects of climate change on an important natural and planted forest tree species.

This approach has considerable utility as a method of partitioning the direct and indirect effects (e.g. mediated by diseases and insects) of climate change on the potential distributions of dominant forest trees. Our research shows that the indirect influences of climate change mediated through disease are an important consideration for planning location of future plantations. For the example shown, direct impacts of climate change on temperature and soil moisture markedly reduce the biological range of Douglas-fir in the North Island. The commercial range of Douglas-fir (as defined here as areas with $F_{ret} > 60\%$) is then further limited, within this delineated area, by the indirect impacts of increasing disease severity. Under the least conservative climate change scenario (NCAR under the A2 emission scenario), projected reductions in the commercial range of Douglas-fir suggest the North Island will be largely unsuitable for the species by the end of this century.

The strong relationship found here between the CLIMEX GI and both pathogen abundance and disease severity accords broadly with previous research. Previous approaches have demonstrated CI to be most strongly related to winter air temperature, spring rainfall and duration of leaf wetness over summer (Manter *et al*., 2005; Stone *et al*., 2007). Needle retention has been found to be strongly and negatively related to CI (Stone *et al*., 2007). This relationship reflects the sensitivity of foliage retention to these environmental drivers, with foliage retention declining under warmer wet conditions, as the CI increases (Manter *et al*., 2005; Stone *et al*., 2007).

Growth index in CLIMEX includes similar explanatory variables, as it is derived from the combination of air temperature and water balance. Within CLIMEX neither precipitation nor leaf wetness are available as direct outputs. Some researchers consider use of water balance as a surrogate for leaf wetness a weakness, particularly for pathogens that require leaf wetness for infection (e.g. Pivonia & Yang, 2004). However, it is worth noting that satisfactory CLIMEX models for foliar pathogens, in which leaf wetness is critical for infection, have been previously developed (e.g. Yonow *et al*., 2004). Leaves can be wetted by rain or dew, which forms under high (>90%) relative humidity (Wallin, 1963). At coarser temporal and spatial scales, sufficient to describe the general climatic suitability for establishment of a pathogen, relative humidity and precipitation are correlated (Chtioui *et al*., 1999; Thornton *et al*., 2000).

Although environmental drivers of disease are similar to those used for modelling other pathosystems, the underlying climatology and functions used for estimating foliage retention differs between CLIMEX and previous approaches. The CLIMEX model is formulated using principles that accord with little known, but powerful, longstanding ecological tenets: the Sprengel–Liebig Law of the Minimum (reviewed in van der Ploeg *et al*., 1999) and Shelford's Law of Tolerance (reviewed in Shelford, 1963). This approach is more mechanistic than previous methods that use multiple regression models, and lends itself not only to properly portraying potential geographical range but also to phenological growth pattern. One limitation of the CLIMEX approach is that the functions assume disease development to be sensitive to meteorology over the entire year, when in practice, often development is most constrained by meteorology over a defined seasonal time period. Severity of Swiss needle cast has been previously shown to be most sensitive to winter air temperature and spring or summer rainfall. However, in support of our approach, a comparison using the dataset described here, shows the CLIMEX GI accounts for more of the variance in foliage retention than empirical models with these seasonally based monthly averages ($R^2 = 0.61$ vs. 0.47, data not shown). Although coefficient of determination should not be viewed as the ultimate arbitrator of model performance, this comparison does at least suggest the CLIMEX approach to be reasonably robust for Swiss needle cast.

Estimation of foliage retention and pathogen abundance from the same independent variables has a sound basis for the pathogen studied here. Fruiting bodies (pseudothecia) of *P. gaeumannii* physically occlude the stomata of Douglas-fir needles, thereby impairing gas exchange and photosynthesis (Manter *et al*., 2003). The premature loss of foliage and resulting growth reduction in Douglas-fir are thus directly related to a decrease in CO_2 assimilation that in turn is directly linked to the abundance of the pathogen (Manter *et al*., 2003). This relationship has been convincingly demonstrated in both Oregon and New Zealand using the proportion of occluded stomata as a measure of pathogen abundance and host needle retention to quantify foliage loss (Hood & Kimberley, 2005; Stone *et al*., 2007, 2008a). Given the strong relationship between pathogen abundance and needle retention, it follows that these variables will be sensitive to the same environmental drivers.

As well as being correlated to pathogen abundance, needle retention has been found to be the most important determinant of reductions in tree volume (Maguire *et al*., 2002). Consequently, our projections of foliage retention under current climate broadly agree with previous research describing how the disease spatially reduces Douglas-fir volume within New Zealand. Kimberley *et al.* (2011) demonstrated volume losses, attributable to increasing disease, increase with air

temperature with average reductions of 34.6% in the North Island and 22.9% in the South Island.

Given the relationship between foliage retention and tree volume, it is not surprising that areas with foliage retention >60% closely correspond to the commercial range of Douglas-fir plantations in New Zealand. The majority of Douglas-fir plantations (76%, 82 799 ha) are located in the South Island, where all locations are projected to have $F_{ret} > 60\%$. Similarly, the majority (57%) of the North Island resource (26 682 ha), occurs at high altitude, where F_{ret} ranges from 60% to 90% under current climate. In Auckland and Northland, where F_{ret} is <60%, stands cover only 32 ha or 0.029% of the total New Zealand estate. Similarly, very little of the Douglas-fir resource is located in coastal areas in Gisborne, Bay of Plenty and Waikato, in which $F_{ret} < 60$.

Our results suggest that climate change is likely to have the greatest impact on foliage retention and productivity of Douglas-fir in the North Island. These results agree with previous research that has projected future disease severity using a more empirical model (Watt *et al*., 2010). By 2090, reductions in F_{ret} are very marked, and particularly within the North Island using projections from the NCAR and MIROC models. Under all six scenarios, areas with $F_{ret} > 60\%$ in the North Island reduce by an average of 68% (range 40–87%). Assuming the worst case scenario is good practice in risk planning, and reasonably likely given recent recorded global warming (Rahmstorf *et al*., 2007) and the lack of political progress towards limitation of greenhouse gases. Under this worse case scenario (NCAR A2) most of the North Island is likely to be unsuitable or at best marginal, for Douglas-fir by the end of this century. Within the South Island, reductions in F_{ret} attributable to increasing air temperature are dampened, as the proportion of high elevation sites with air temperature below the threshold for foliage loss is greater than in the North Island. Apart from coastal and low lying regions, large areas within the South Island are projected to sustain relatively low levels of disease, and remain suitable for Douglas-fir under all scenarios. Global warming may also provide some opportunity to extend the species range into higher altitude South Island areas that were previously unsuitable for Douglas-fir.

This case study illustrates the importance that high impact pests could have on the future composition of both planted and native forests. For tree species suited to a particular climatic zone, the direct effects of changing climate (e.g. temperature and CO_2) might be expected to similarly influence growth of different tree species. However, as insects and diseases are often host specific, they are likely to differentially affect species growth rates, and could thus have a major bearing on future species composition. Our results show changes in disease severity could markedly impact the suitability of areas for plantation grown Douglas-fir. Similarly, in native forests, the effects of climate change on populations of host-specific pathogens or insect pests could affect interspecific competition and result in changes in dominance and distribution. Thus, assuming sufficient biological knowledge, the impact of pest and diseases on forests under changing environmental conditions should be an integral feature of climate change prediction models.

The approach taken here has considerable potential as a generic method of predicting pest impacts on long lived, high value crop species under both current and future climate. The method is particularly applicable to diseases of plantation species that show sensitivity to environment. Dothistroma needle blight, one of the most damaging diseases of *Pinus* spp., may provide a useful further case study. Severity of this disease has been successfully modelled at broad scales across New Zealand using air temperature, rainfall and relative humidity (Watt *et al*. 2011). As with Swiss needle cast, needle loss resulting from Dothistroma needle blight is strongly related to reduction in volume growth (van der Pas, 1981).

The key advance of the approach outlined here is that spatial variation in disease impacts are constrained to areas that are modelled as being suitable for both the host and pest. Using this method, there is a requirement for high quality data describing a symptom of disease severity that directly impacts the host and is sensitive to climate. Although this requirement is relatively demanding, results shown here demonstrate the importance of integrating biotic factors into models that describe the impacts of climate change on plantation species distribution. Failure to do so could result in predictions that do not adequately represent future plantation growth and distribution.

Acknowledgements

Technical, administrative or other support was provided by: Len Coop, Judy Gardner, Sam Hendrick, Rachel Hood, Nick Ledgard, Charlie Low, Tod Ramsfield, Daphne Stone and Wendy Sutton.

References

Black BA, Shaw DC, Stone JK (2010) Impacts of Swiss needle cast on overstory Douglas-fir forests of the western Oregon Coast Range. *Forest Ecology and Management*, **259**, 1673–1680.

Boyce JS (1940) A needle-cast of Douglas fir associated with *Adelopus gäumanni*. *Phytopathology*, **40**, 649–659.

Brasier CM, Scott JK (1994) European oak declines and global warming: a theoretical assessment with special reference to the activity of *Phytophthora cinnamomi*. *EPPO Bulletin*, **24**, 221–232.

Chtioui Y, Francl LJ, Panigrahi S (1999) Moisture predictions from simple micrometeorological data. *Phytopathology*, **89**, 668–672.

Coakley SM, Scherm H, Chakraborty S (1999) Climate change and disease management. *Annual Review Phytopathology*, **37**, 399–426.

De Wolf ED, Isard SA (2007) Disease cycle approach to plant disease prediction. *Annual Review of Phytopathology*, **45**, 203–220.

Desprez-Loustau ML, Robin C, Reynaud G *et al.* (2007) Simulating the effects of a climate-change scenario on the geographical range and activity of forest-pathogenic fungi. *Canadian Journal of Plant Pathology*, **29**, 101–120.

Ganley RJ, Watt MS, Manning L *et al.* (2009) A global climatic risk assessment of pitch canker disease. *Canadian Journal of Forest Research*, **39**, 2246–2256.

Hansen EM, Stone JK, Capitano BR *et al.* (2000) Incidence and impact of Swiss needle cast in forest plantations of Douglas-fir in coastal Oregon. *Plant Disease*, **84**, 773–778.

Hood IA, Kimberley MO (2005) Douglas fir provenance susceptibility to Swiss needle cast in New Zealand. *Australasian Plant Pathology*, **34**, 57–62.

Hood IA, Sandberg CJ, Barr CW *et al.* (1990) Changes in needle retention associated with the spread and establishment of *Phaeocryptopus gaeumannii* in planted Douglas fir. *European Journal of Forest Pathology*, **20**, 418–429.

Kimberley MO, Hood IA, Knowles RL (2011) Impact of Swiss needle-cast on growth of Douglas-fir. *Phytopathology*, **101**, 583–593.

Kirschbaum MUF, Mason NWH, Watt MS *et al.* (2010) *Productivity Surfaces for Pinus radiata and a Range of Indigenous Forests Under Current and Future Climatic Conditions*. MAF report. Ministry of Agriculture and Forestry, Wellington, New Zealand.

Kriticos DJ, Alexander NS, Kolomeitz SM (2006) Predicting the potential geographic distribution of weeds in 2080. In Fifteenth Australian Weeds Conference Weed Science Society of Victoria, Adelaide, Australia, pp. 27–34.

Lanoiselet V, Cother EJ, Ash GJ (2002) Climex and Dymex simulations of the potential occurrence of rice blast disease in south-eastern Australia. *Australasian Plant Pathology*, **31**, 1–7.

Maguire DA, Kanaskie A, Voelker W *et al.* (2002) Growth of young Douglas-fir plantations across a gradient in Swiss needle cast severity. *Western Journal of Applied Forestry*, **17**, 86–95.

Manter DK, Bond BJ, Kavanagh KL *et al.* (2003) Modelling the impacts of the foliar pathogen, *Phaeocryptopus gaeumannii*, on Douglas-fir physiology: net canopy carbon assimilation, needle abscission and growth. *Ecological Modelling*, **164**, 211–226.

Manter DK, Reeser PW, Stone JK (2005) A climate-based model for predicting geographic variation in Swiss needle cast severity in the Oregon Coast Range. *Phytopathology*, **95**, 1256–1265.

Marks GC, Smith IW, Cook IO (1989) Spread of *Dothistroma septospora* in plantations of *Pinus radiata* in Victoria between 1979 and 1988. *Australian Forestry*, **52**, 10–19.

Meehl GA, Covey C, Delworth T *et al.* (2007) The WCRP CMIP3 multimodel dataset: a new era in climate change research. *Bulletin of the American Meteorological Society*, **88**, 1383–1394.

Mitchell TD, Carter TR, Jones PD *et al.* (2004) *A Comprehensive Set of Climate Scenarios for Europe and the Globe: the Observed Record (1900-2000) and 16 Scenarios (2000-2100)*. University of East Anglia, Working Paper 55.

Morton HL, Patton RF (1970) Swiss needlecast of Douglas fir in the Lake States. *Plant Disease Reporter*, **54**, 612–616.

van der Pas JB (1981) Reduced early growth rates of *Pinus radiata* by *Dothistroma pini*. *New Zealand Journal of Forestry Science*, **11**, 210–220.

Paul I, Van Jaarsveld AS, Korsten L *et al.* (2005) The potential global geographical distribution of citrus black spot caused by *Guignardia citricarpa* (Kiely): likelihood of disease establishment in the European Union. *Crop Protection*, **24**, 297–308.

Peace TR (1962) *Pathology of Trees and Shrubs, with Special Reference to Britain*. Clarendon Press, Oxford, England.

Pennycook SR (1989) *Plant Diseases Recorded in New Zealand*, **Vol 3**. Plant Diseases Division, D.S.I.R., Auckland, New Zealand.

Pivonia S, Yang XB (2004) Assessment of the potential year-round establishment of soybean rust throughout the World. *Plant Disease*, **88**, 523–529.

van der Ploeg RR, Bohm W, Kirkham MB (1999) On the origin of the theory of mineral nutrition of plants and the law of the minimum. *Soil Science Society of America Journal*, **63**, 1055–1062.

Pradhan S (1946) Insect population studies. IV. Dynamics of temperature effect on insect development. *Proceedings of the National Institute of Science India*, **12**, 395–404.

Rahmstorf S, Cazenave A, Church JA *et al.* (2007) Recent climate observations compared to projections. *Science*, **316**, 709.

Shelford VE (1963) *The Ecology of North America*. University of Illinois Press, Urbana, IL.

Stinner RE, Gutierrez AP, Butler GD (1974) An algorithm for temperature-dependent growth rate calculation. *The Canadian Entomologist*, **106**, 519–523.

Stone JK, Hood IA, Watt MS *et al.* (2007) Distribution of Swiss needle cast in New Zealand in relation to winter temperature. *Australasian Plant Pathology*, **36**, 445–454.

Stone JK, Capitano BR, Kerrigan JL (2008a) The histopathology of *Phaeocryptopus gaeumannii* on Douglas-fir needles. *Mycologia*, **100**, 431–444.

Stone JK, Coop LB, Manter DK (2008b) Predicting effects of climate change on Swiss needle cast disease severity in Pacific Northwest forests. *Canadian Journal of Plant Pathology-Revue Canadienne de Phytopathologie*, **30**, 169–176.

Sutherst RW, Maywald GF (1985) A computerised system for matching climates in ecology. *Agriculture, Ecosystems and Environment*, **13**, 281–299.

Sutherst RW, Maywald GF, Kriticos DJ (2007) *CLIMEX Version 3: User's Guide*. Hearne Scientific Software Pty Ltd. Available at: http://www.Hearne.com.au.

Temel F, Stone JK, Johnson GR (2003) First report of Swiss needle cast caused by *Phaeocryptopus gaeumannii* on Douglas-fir in Turkey. *Plant Disease*, **87**, 1536.

Thornton PE, Hasenauer H, White MA (2000) Simultaneous estimation of daily solar radiation and humidity from observed temperature and precipitation over complex terrain in Austria. *Agricultural Forest Meteorology*, **104**, 255–271.

Venette RC, Cohen SD (2006) Potential climatic suitability for establishment of *Phytophthora ramorum* within the contiguous United States. *Forest Ecology and Management*, **231**, 18–26.

Wallin JR (1963) Dew, its significance and measurement in phytopathology. *Phytopathology*, **53**, 1210–1216.

Wallin JR, Waggoner PE (1950) The influence of climate on the development and spread of *Phytophthora infestans* in artificially inoculated potato plots. *Plant Disease Reporter Supplement*, **190**, 19–33.

Watt MS, Kriticos DJ, Alcaraz S *et al.* (2009) The hosts and potential geographic range of Dothistroma needle blight. *Forest Ecology and Management*, **257**, 1505–1519.

Watt MS, Palmer DJ, Bulman LS (2011) Predicting the severity of Dothistroma on *Pinus radiata* under current climate in New Zealand. *Forest Ecology and Management*, **261**, 1792–1798.

Watt MS, Stone JK, Hood IA *et al.* (2010) Predicting the severity of Swiss needle cast on Douglas fir under current and future climate in New Zealand. *Forest Ecology and Management*, **260**, 2232–2240.

Wharton TN, Kriticos DJ (2004) The fundamental and realized niche of the Monterey Pine aphid, *Essigella californica* (Essig) (Hemiptera**:** Aphididae): implications for managing softwood plantations in Australia. *Diversity and Distributions*, **10**, 253–262.

Whetton PH, McInnes KL, Jones RN *et al.* (2005) *Australian Climate Change Projections for Impact Assessment and Policy Application: A Review*. CSIRO Marine and Atmospheric Research, Paper No. 1, Melbourne, Australia.

Yonow T, Kriticos DJ, Medd RW (2004) The potential geographic range of *Pyrenophora semeniperda*. *Phytopathology*, **94**, 805–812.

Supporting Information

Additional Supporting Information may be found in the online version of this article:

Figure S1. Map of the world showing the distribution of growth index, GI_A, for regions with ecoclimatic index, EI > 0. Areas shown as white are unsuitable (EI = 0) for the disease or host. Also shown is the distribution of Swiss needle cast, shown as point locations (red circles) and provincial records (cross-hatched areas), in which at least one observation has been recorded.

Please note: Wiley-Blackwell are not responsible for the content or functionality of any supporting materials supplied by the authors. Any queries (other than missing material) should be directed to the corresponding author for the article.